

Application of Genetic Algorithms to an Inverse Field Problem in Magnetic Fluid Dynamics

Milko Kuilekov¹, Marek Ziolkowski^{1,2}, Hartmut Brauer¹

Abstract: The purpose of the present work is to study whether genetic algorithms can solve an inverse field problem in magnetic fluid dynamics (MFD) efficiently. We have investigated how the interface between two fluids of different conductivity in a highly simplified model of an aluminum electrolysis cell can be reconstructed by means of external magnetic field measurements. The knowledge of the interface deformation can be used to prevent undesired instabilities in aluminum reduction cells [1].

Keywords: Genetic algorithm, Optimisation simulations, Inverse solution, Interface reconstruction.

1 Introduction

Genetic algorithms (GAs) – search techniques based on the mechanism of natural evolution and genetics – become more and more popular to solve optimisation problems. GAs can solve a broad spectrum of problems, from traditional optimisation in engineering to inverse field problems in MFD and financial prediction in economics. GAs has been shown to solve linear and non-linear problems by exploring all regions of the state space and exploiting promising areas through mutation, crossover, and selection operations [2, 3].

The basic idea of our research is to exploit different GAs and their parameters in order to obtain precise solution and efficiency of computation process. We have demonstrated that the external magnetic field generated by the electrical current flowing through a highly simplified model of an aluminum reduction cell provides sufficient information to reconstruct the unknown interface shape. GA generates the inverse field solution on the base of evaluation of the forward solution.

2 Problem Definition

Two fluids with different electrical conductivities are situated in a long cylinder with radius R (Fig.1). The cylinder walls are non-conducting. Along the length axis of the cylinder a homogeneous electrical current density \mathbf{J}_0 is applied. If the interface between the fluids is flat, the current density \mathbf{J} is homogeneous everywhere. As soon as

¹ Technische Universitaet Ilmenau, Helmholtzplatz 2, D-98684 Ilmenau, Germany
e-mail: milko.kuilekov@tu-ilmenau.de

² Technical University of Szczecin, Sikorskiego 37, PL-70313 Szczecin, Poland

the interface deviates from its flat shape due to interfacial waves or an external forcing, the current density will become inhomogeneous near the interface. If the perturbation of the fluid interface is non axisymmetric, it leads to a perturbation of the magnetic field outside the cylinder. This fact is used for the interface reconstructions. Impressed current is $I = 1$ A, conductivity of fluid 1 is $\gamma_1 = 100$ S/m and conductivity of fluid 2 is $\gamma_2 = 3.6 \times 10^6$ S/m.

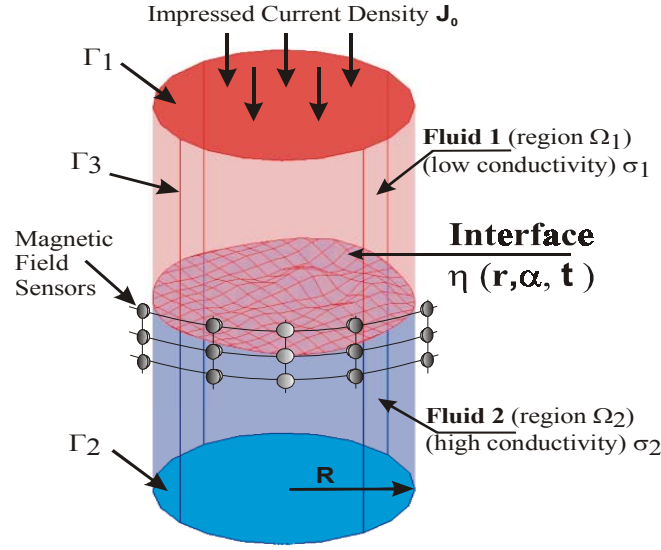


Fig. 1 – Simplified model of aluminum reduction cell.

2.1 Basic Dependencies

Interface perturbation is expressed by Bessel and trigonometric functions [4] and has the form

$$\eta(r, \alpha) = A \cdot \sum_{m=-M}^M \sum_{n=1}^N \kappa_{mn} \cdot J_m(k_{mn} \cdot r) \cdot e^{jm \cdot \alpha}, \quad (1)$$

where r and α are the radial and azimuthal coordinates, J_m is a Bessel function of the first kind, $k_{mn} = r_{mn}/R$, r_{mn} is the n -th solution of the equation $J'_m(r) = 0$ at $m > 0$, n is the radial mode number and m is the azimuthal mode number, κ_{mn} is a weight coefficient of mode (m, n) and A is a scaling factor of the amplitude.

The magnetic field is obtained using the current density perturbation and the Biot–Savart law. Electrical potential perturbation in the fluids is described as [3]

$$\varphi_i(r, \alpha, z) = \text{sign}(z) \cdot \frac{J_0}{\gamma_i} \cdot \frac{\gamma_1 - \gamma_2}{\gamma_1 + \gamma_2} \cdot \eta(r, \alpha) \cdot e^{-k_{mn}|z|}, \quad (2)$$

where J_0 is the impressed current density, γ_1 and γ_2 are the conductivities of fluids.

Current density perturbation is calculated from

$$\mathbf{j} = -\gamma \cdot \nabla \varphi . \quad (3)$$

Applying the Biot–Savart law, the magnetic flux density perturbation is received from the equation

$$\mathbf{b}(\mathbf{r}) = \frac{\mu_0}{4\pi} \iiint_{(V')} \frac{\mathbf{j} \times (\mathbf{r} - \mathbf{r}')}{|\mathbf{r} - \mathbf{r}'|^3} dV' . \quad (4)$$

2.1 Simple Genetic Algorithm Solver

A block diagram of the simple genetic algorithm optimiser is presented in Fig.2. The inverse solver consists of three main parts: *Initialisation*, *Evaluation* and *Simple GA*. The *Initialisation* block is responsible for setting the GA parameters, defining the representation scheme as it is discussed further, and for generating the initial solution. The *Evaluation* block contains the forward solution of the field problem as it is discussed in the previous section. Forward sub-block forms the magnetic field distribution, evaluated in the cost function sub-block. *Simple GA* generates the variables vector defining the interface shape used from the forward solver at each iteration.

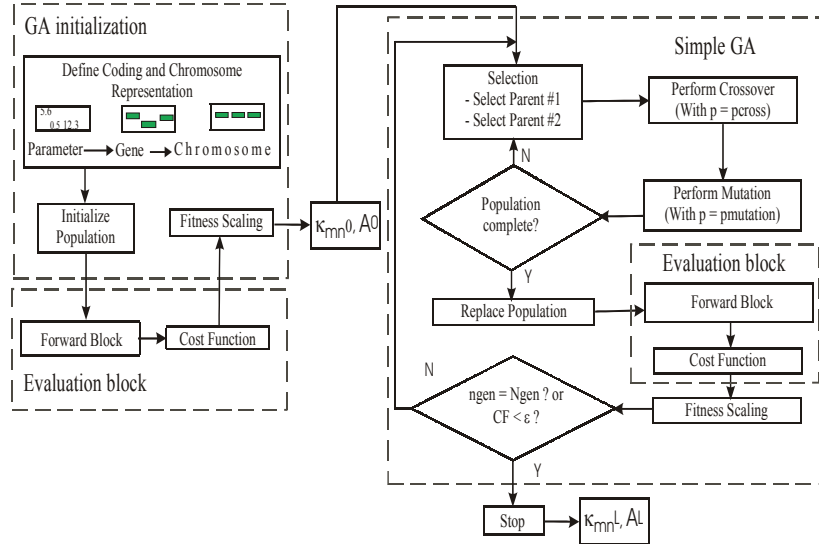


Fig. 2 – Block diagram of a Simple GA loop for obtaining the inverse solution.

2.2 Simple GA

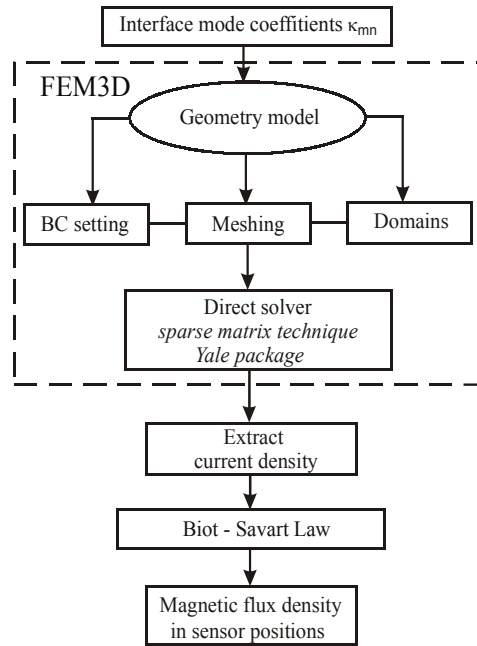


Fig. 3 – Block diagram representing the forward solution calculations.

The use of a genetic algorithm requires the determination of six fundamental issues: chromosome representation, selection function, the genetic operators making up the reproduction function, the creation of initial population, termination criteria, and the cost function. The representation scheme determines how the problem is structured in the GA and also determines the genetic operators that are used. Each individual or chromosome is made up of a sequence of genes from a certain alphabet. An alphabet could consist of binary digits, floating point numbers, integers, symbols, matrices, etc. The selection of individuals to produce successive generations plays an extremely important role in a genetic algorithm. A probabilistic selection is performed based upon the individual's fitness such that the better individuals have an increased chance of being selected. There are several schemes for the selection process: roulette wheel selection and its extensions, scaling techniques, tournament, elitism models, and ranking methods. Genetic operators provide the basic search mechanism of the GA. The operators are used to create new solutions based on existing solutions in the population. There are two basic types of operators: crossover and mutation. Crossover takes two individuals and produces two new individuals while mutation alters one individual to produce a single new solution. The application of these two basic types of operators and their derivatives depends on the used chromosome representation. The GA requires an initial population. The most common method is to generate solutions for the entire population randomly. The beginning population can be seeded with potentially good solutions. The GA moves from generation to generation selecting and reproducing parents until a termination crite-

tion is met. The most frequently used stopping criterion is a specified maximum number of generations. The cost function is formed from an evaluation block (Fig.2) connected to the solved problem and independent of the GA. The cost (objective) function represents current solution goodness. In the simple genetic algorithm the new generation has the same size as the current generation, which is completely replaced.

2.3 Forward Block

In Fig.3 is represented the *Forward Block* diagram. The main purpose of the shown solver is to form a magnetic induction template corresponding to a certain interface description. For forward calculations we have used finite element program - *FEM3D* [5] combined with calculations for the magnetic field in certain positions around the cylinder. The finite element mesh with 27707 nodes and 123200 tetrahedrons is shown in Fig.4.

Weight coefficients κ_{mn} described in *Basic Dependencies* section are used as input variables for the FEM program. From the input vector variables and a set of geometrical and physical constants is formed the geometry model of the cell. Output of the FEM module is a set of current density dipoles calculated for a finite number of points from the cylinder volume. The extracted current density is used from the next program sub-blocks, which include *Biot-Savart Law* calculations and magnetic flux density distribution in certain predefined number of points around the cell.

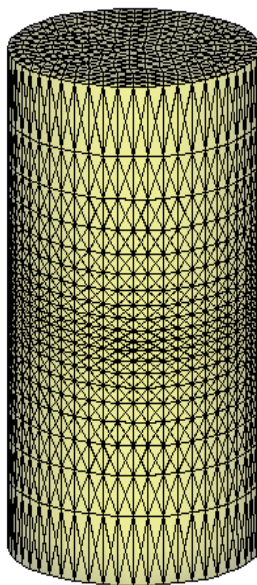


Fig. 4 – *Finite element method mesh of the cylinder.*

2.4 Inverse problem strategy

The magnetic flux density measured in several positions located on concentric rings around the cylinder is used to identify the interface (Fig.1). In our computation case we have presumed that the fluctuating interface is in a steady state, i.e. we choose the time moment in which the measured signal has a maximal value. Genetic algorithm is used together with the forward solution (Fig.3) in a computation loop (Fig.2). GA generates current interface reconstruction parameters κ_{mn} , according to evolution principles. The procedure is repeated until the objective function reaches predefined stopping criteria. For our computations we have applied a C++ library of genetic algorithm components (GAlib) developed at the M. I. T. [6].

The cost (objective) function (CF) is defined as a sum of differences between measured (parametric) and computed magnetic flux density components b_r and b_z ,

$$CF = \sum_{i=1}^N \sqrt{(b_{rm}^{(i)} - b_r^{(i)})^2 + (b_{zm}^{(i)} - b_z^{(i)})^2}, \quad N = NP \cdot NR, \quad (5)$$

where NP is the number of sensors in row and NR is the number of rows.

3 Computation parameters. Simple GA optimisation results

In the considered case a fixed scaling amplitude $A = 2.5$ mm and 9 weight coefficients κ_{mn} encoded by GA like binary strings have been used. The first experimental implementation of the studied problem will be conducted with 1 sensor row of 8 sensors uniformly distributed around the cylinder. The distance between the sensors and the wall of the cell is 10 mm. According that for our computations we have used the same sensor (template) ring situated in the middle of the cylinder (Fig.7). As an example, we have reconstructed the shape of the interface described by a hybrid mode: $\eta_{13} + \eta_{22}$ (Fig.5). Magnetic flux density obtained from the considered sensor template has component $b_z = 0$. The interface has been reconstructed only from component b_r measured in 8 sensor points. The corresponding magnetic field is shown in Fig.6.

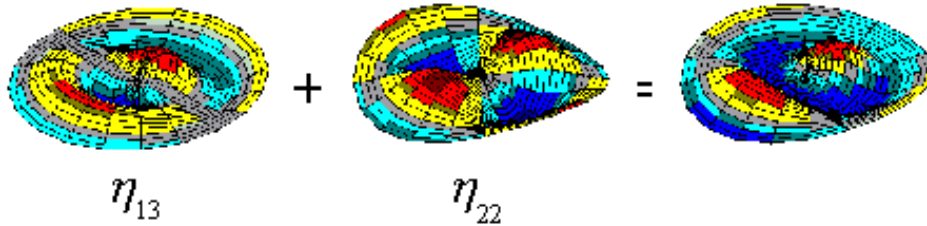


Fig. 5 – Constitution of the examined test mode.
The sample interface is a superposition of two single interface modes.

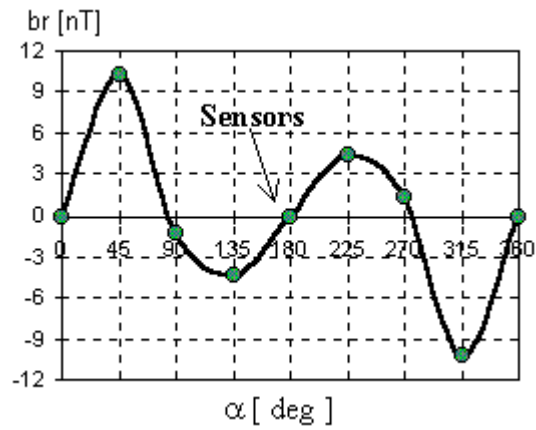


Fig. 6 – Magnetic flux density component b_r , simulated for hybrid mode $\eta_{13} + \eta_{22}$ with 8 sensors at $z = H/2$, where H is cylinder height.

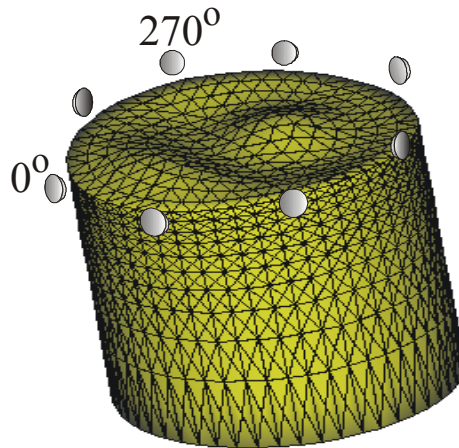


Fig.7 – Magnetic sensor positions according domain 2 of the cell.

3.1 GA Parameters

The population size consists of 40 individuals. Binary strings of 16 bits length are allocated to represent each variable, yielding to a chromosome length of 144 bits per individual. GA has maximized negative value of fitness function, i.e. has minimized the cost function value. As a scaling scheme a sigma truncation fitness has been used. The sigma truncation scaling scheme is defined as:

$$f_{scaled} = \begin{cases} f' = f - (\bar{f} - c \cdot f_{dev}) & \text{if } f' \geq 0 \\ 0 & \text{otherwise} \end{cases}, \quad (6)$$

where $f = -CF$ is fitness value, \bar{f} is the population average fitness and f_{dev} is a measure of the deviation of the fitness value from the average value. Proportional selection strategy (roulette wheel selection) has been used. The probability of selecting an individual from a population is purely function of relative fitness of the individual. One point crossover has been applied with an occurrence probability $p_c = 0.95$ per chromosome pair. The mutation probability was $p_m = 0.01$. Elitism strategy has been also chosen, because the best individual from each generation has been copied to the next generation.

3.2 Computation results

Optimization run of 100 generations has been performed. An objective function convergence curve is shown in Fig.8. It can be seen that between 50th and 70th generations the cost function value remains unchanged. That undesired effect is called premature convergence. The quality of the solution is evaluated by the difference between exact and reconstructed interface, defining the reconstruction error

$$\Delta z = \sqrt{\frac{\sum_{i=1}^k (z_i - z'_i)^2}{\sum_{i=1}^k z_i'^2}} \cdot 100, \% , \quad (7)$$

where k is a finite number of points, z'_i is the exact interface coordinate at point i and z_i is the reconstructed interface coordinate at point i . Reconstruction error versus the generation number is shown in Fig.9. After 100 generations, for $k = 441$ and $CF = 2$ nT, the reconstruction error is $\Delta z = 9$ %. The reconstructed and the exact interface are shown in Fig.10. It is obvious that simple GA fails in finding interface shape. That is explained as a convergence to a suboptimal point.

If some of the average individuals have extraordinary fitness, the mechanism of GAs may lead to a premature convergence, which is defined as a convergence to a suboptimal solution.

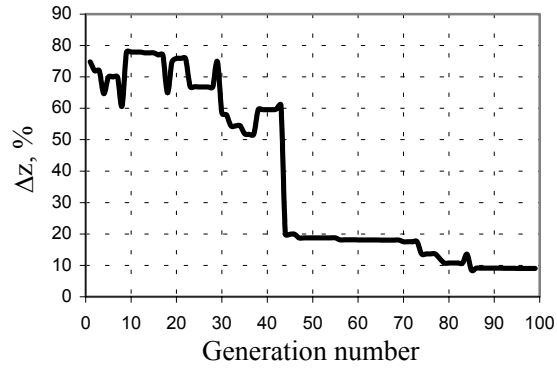


Fig. 8 – Convergence curve of Simple GA optimization loop

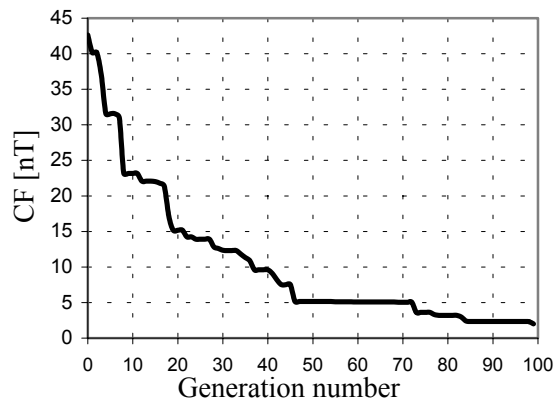


Fig. 9 – Reconstruction error versus generations of Simple GA optimisation loop.

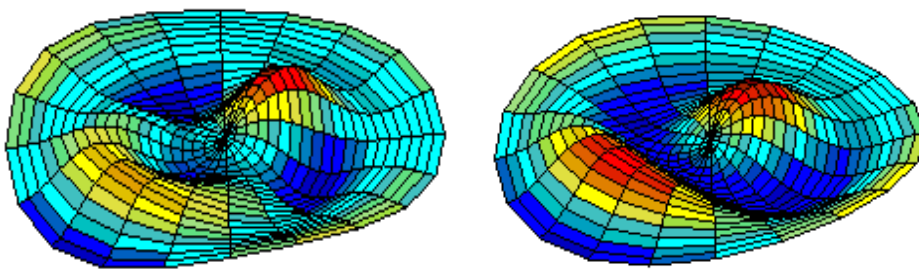


Fig. 10 – Exact (left) and reconstructed (right) interfaces. Simple GA.

4 Multi – loop GA

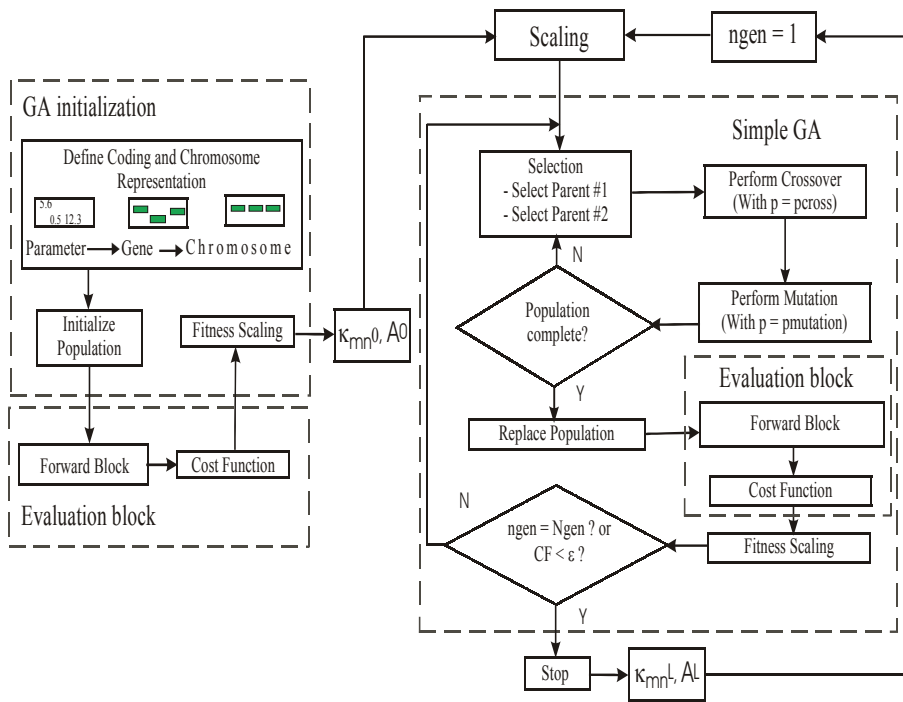


Fig. 11 – Block diagram of a multi – loop genetic algorithm optimizer.

The problem of the premature convergence discussed in the previous section can be avoided by applying multiple, optimisation loop. A block diagram of such multi – loop GA is shown in Fig.11. In multiple loops the simple GA is used in several consecutive runs. The loop consists of the already known *GA Initialisation* and *Simple GA* blocks and of a *Scaling* block (Fig.12). The purpose of the *Scaling* block is to re-scale the initial vector of each simple GA run to the last vector obtained from the previous run. In that sense, starting point for each run is the same but the variable vectors are scaled to the last point from the run before.

4.1 Precision of the solution and comparison

Computation process has been performed with the same GA parameters discussed in *GA parameters* section. Two consecutive runs of 50 generations each have been applied. The number and position of sensors were the same as in the previous section and the hybrid mode $\eta_{13} + \eta_{22}$ was reconstructed. The computation results are compared to those of the simple GA run. Cost function convergence curves are shown in Fig.13. It is seen that up to 50 generations multi – loop and simple GA run curves match and after 50 generations the multi – loop curve has continued going down to the optimal cost function

value. Thus the problem of premature convergence has been overcome. Reconstruction error versus generations is shown in Fig.14. After 2 times 50 generations, for $k = 441$ and $CF = 0.11$ nT, the reconstruction error is $\Delta z = 0.36$ %, i.e. a much higher precision was achieved. Reconstructed and exact interface are shown in Fig.15.

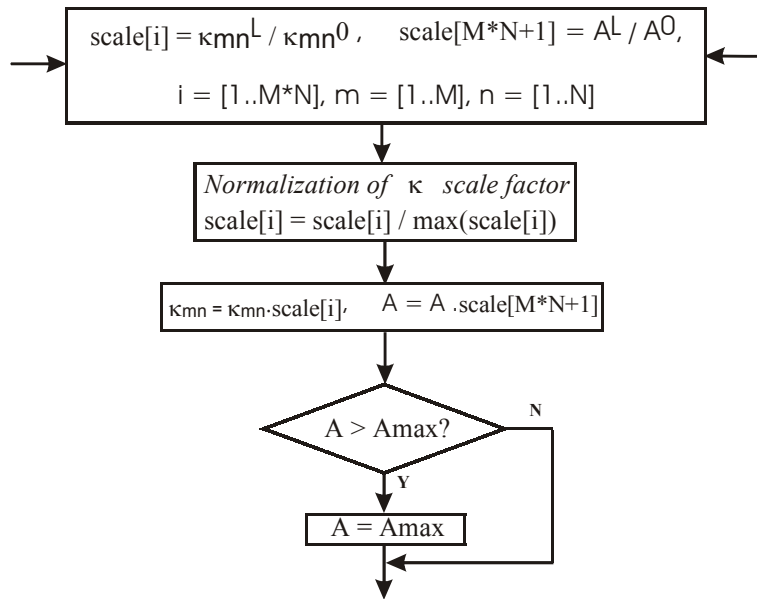


Fig. 12 – Scaling Block.

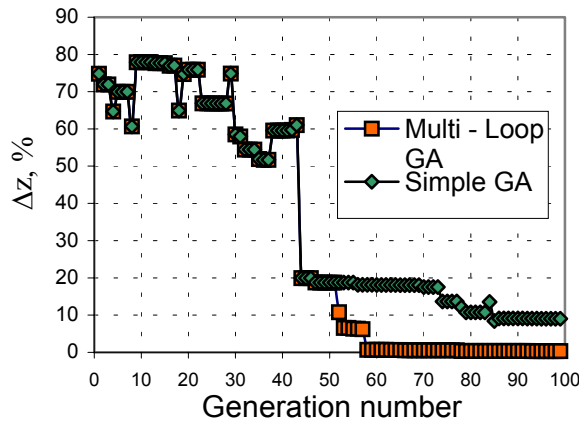


Fig. 13 – Convergence curves of Mult Loop and Simple GA.

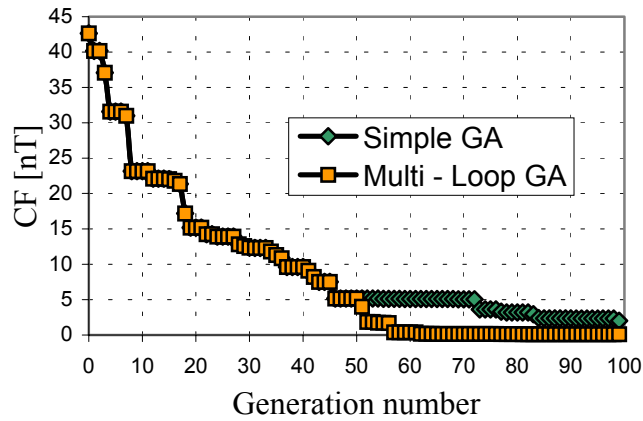


Fig. 14 – Reconstruction error versus generations of Multi – Loop and Simple GA.

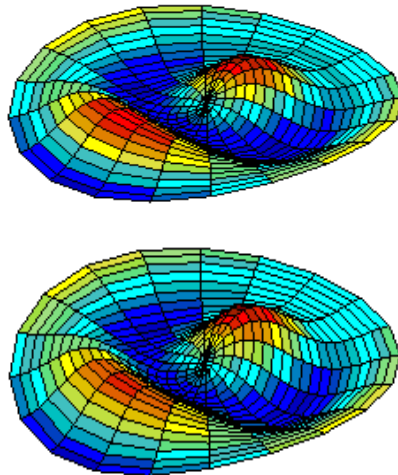


Fig. 15 – Exact(left) and reconstructed(right) interfaces for the Multi – Loop GA optimization run.

5 Conclusions

The predefined interface between the two conducting fluids was reconstructed with high precision from flux density component b_r obtained from 8 sensors situated in the middle plane around the cylinder. The Simple GA loop solution fails because of its local convergence. Multiple GA loop that includes Simple GA loop inside avoids premature convergence and minimizes the cost function to very low values corresponding to a reconstruction with high precision.

References

- [1] A. Kurenkov, A. Thess: Reconstruction of interfaces between electrically conducting fluids from electrical potentials measurements, 4th Int. Conf. Of Magnetohydrodynamics, Giens/France, September 2000, Proc. Vol. 1, pp. 45 - 50, 2000.
- [2] Y. Rahmat-Samii, E. Michielssen: Electromagnetic Optimisation by Genetic Algorithms, Wiley, 1999.
- [3] Z. Michalewicz: Genetic Algorithms + Data Structures = Evolution Programs, 3rd ed., Springer Verlag, Berlin, Heidelberg, New York, 1996.
- [4] H. Brauer, M. Ziolkowski, M. Danneman, M. Kuilekov, D. Alexeevski: Forward Simulations for Free Boundary Reconstruction in Magnetic Fluid Dynamics, COMPEL, Vol. 1, 2003.
- [5] M. Gramz, M. Ziolkowski: Calculation of 3D electromagnetic fields, PN Technical University of Szczecin, Poland, No 444, 1991 (in polish).
- [6] M. Wall Galib: A C++ Library of Genetic Algorithm Components, Version 2.4, 1996 (<http://lancet.mit.edu/ga>).